

Simplified Arithmetic Hilbert Transform based Wide-Band Real-Time Digital Frequency Estimator

Jean-Paul Sandoz
University of Applied Sciences
EIAJ-HES, Hôtel de ville 7
2400, Le Locle, Switzerland
Phone ++ 41 32 930 30 30
E-mail: Sandoz@eicn.ch

ABSTRACT

This paper presents a practical solution to the FPGA/CPLD implementation of a Hilbert Transform based real-time frequency estimator. The most important breakthrough of this work is the substitution of the ever-complicated *Arctan* function implementation by the “One-Bit” based balanced *Quadri-Correlator* operating at IF. This has the advantage of producing quasi-instantaneous frequency estimation with no input signal amplitude dependence. The first series of computer simulations show the very good dynamic performances.

Categories and Subject Descriptors

Biomedical -Test and Verification – Non Destructive Structural Testing – Time Evolving Processes Monitoring - Geophysical Apps. - FPGA/CPLD Designs –Sonar, Sonic and Ultrasonic Applications

General Terms

Algorithms, Performance, Design, Theory.

Keywords

FPGA/CPLD – Hilbert Transform – Quadri-Correlator – Multiplication-Free Implementation – Real-Time Frequency Estimator.

1. INTRODUCTION

Vibration analysis of dynamic systems, time-varying characteristics applied to diagnostics, classification based on time evolving system parameters are becoming more important every day. Recently, the availability of powerful digital signal processing software tools prompted resurgence in popularity of developments made decades ago. Recent work [1,2,3] has clearly demonstrated that the Hilbert Transform (HT) has potentialities often overlooked by the practitioners in the past. Even though the HT basic theory and most important properties are well understood and increasingly gaining in attractiveness among the engineering community, their real-time implementation is often rather complex.

The design is based on previous work done by the author [5] and developments made in a diploma work [6]. Without much time devoted to optimization, the preliminary simulations show promising results. The most important characteristics are the followings:

- Frequency range of operation: 200 Hz → 4 kHz
- Low system clock frequency: 80 kHz
- Tracking error standard deviation of slow varying frequency: 3 Hz
- Group delay: 3.0 ms
- 200 Hz to 4 kHz transient time (10% → 90%): 2.5 ms
- Maximum to minimum frequency of operation ratio: 20
- Input signal amplitude insensitive
- Limited “Phase Reversal” effect
- Resistant to wide-band additive background noise
- Very robust to impulsive noise
- Fully controllable frequency estimation accuracy and response time

The overall structure includes the following blocs:

- Multiplication-free all-pass digital filter Hilbert Transformer
- Multiplication-free up-frequency converter
- Single-side band generation at intermediate frequency with IF = 6 → 9.8 kHz
- “One-Bit” based balanced Quadri-Correlator” operating at IF
- Running averagers controlling the frequency estimator dynamic performances

This paper is organized as follows. The basic theoretical analysis is given in Section 2. The details of the proposed multiplication-free solution are presented in Section 3. The simulation results are shown in Section 4. Finally, the last Section summarizes the advantages of this design and suggests potential developments.

2. BASIC THEORETICAL ANALYSIS

Fig. 1 shows the bloc diagram of the complete structure. The input signal $x_{in}(t)$ is an amplitude modulated sine-wave with an instantaneous frequency of $freq_{xin}(t)$ with:

$$200 \text{ Hz} \leq freq_{xin} \leq 4000 \text{ Hz}$$

The Hilbert Transformer output produces an analytic signal $x_{HL}(t)$ defined by:

$$x_{HL}(t) = x_{in}(t) + j\tilde{x}_{in}(t) \text{ where } \tilde{x}_{in}(t) = \mathbf{H}[x_{in}(t)] = x_{in}(t) * (1/j\pi)$$

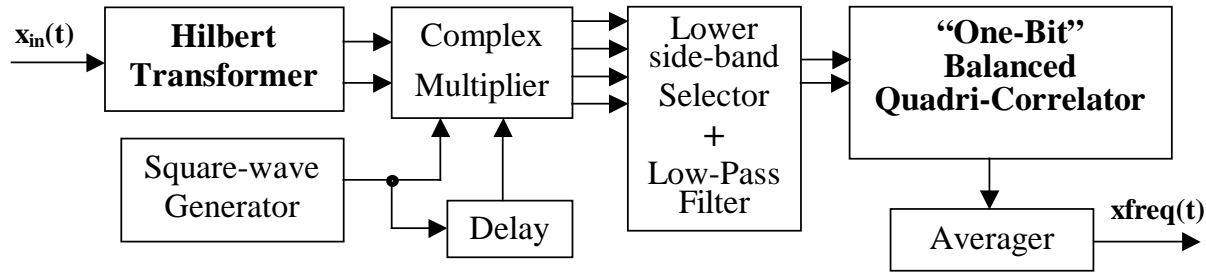


Figure 1 : Bloc diagram of the complete

The square-wave generator output together with the delay element produce a complex carrier with a fundamental frequency $freq_{SQ}$ of 10 kHz. The delay is set at $25 \mu s$ ($1/4f_{SQ}$). The multiplier outputs are combined such that the lower side-band is present in the form of an **analytic signal**. The multiple harmonics generated by the square signal and present on this analytic signal are attenuated by low-pass filters. Furthermore its instantaneous frequency is equal to: $freq_{SQ} - freq_{xin}(t)$.

From Hilbert Transform properties [3] we know that if $y(t)$ is a real function of time, than:

$$\omega(t) = \frac{y(t) \cdot \dot{\tilde{y}}(t) - \dot{y}(t) \cdot \tilde{y}(t)}{A^2(t)}$$

$$A(t) = \sqrt{y^2(t) + \tilde{y}^2(t)}$$

Where $\omega(t)$ and $A(t)$ are the instantaneous frequency and envelope respectively. Then, [5] and [7] point out that the **"One-Bit" balanced Quadri-Correlator** determines the quasi-instantaneous frequency of its input signals.

3. IMPLEMENTATION

3.1 Hilbert Transformer

The Hilbert transformer is realized with three second-order all-pass filters and one unit delay element. Figure 2 shows the structure.

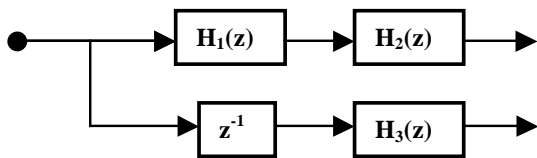


Figure 2 : Hilbert Transformer

It has been determined that some round-off of the coefficients is acceptable. Thus, after running an optimization program [6], the all-pass filters can be expressed in the following form:

$$H_k(z) = \frac{-C_k + 1 \cdot z^{-2}}{1 - C_k \cdot z^{-2}}$$

with $C_k = \pm 2^{-m} \pm 2^{-n}$, m and n (positive integers) ≤ 4

3.2 Complex Multiplier

The square-wave generator, together with the delay bloc provide two components in quadrature at 10 kHz and even harmonic frequencies (i.e. 30, 50 kHz ...) to the first input of the complex multiplier. Its second input comes naturally from the Hilbert transformer outputs. Since the complex multiplier first input has only +1 and -1 as possible values, its implementation reduces down to two's complement arithmetic functions (i.e. multiplication by +1 or by -1).

3.3 Lower Side-Band Selector

The well known phasing technique is then applied to select lower-side band quadrature signals. Figure 3 shows the spectrum obtained after the side-band selection. The desired frequencies, 6 kHz up to 9.8 kHz are more than 10 dB above the strongest unwanted ones.

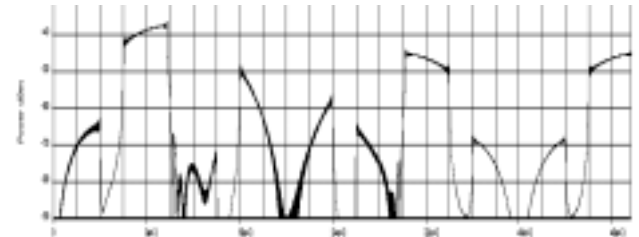


Figure 3 : Lower side-band output spectrum

3.4 Low-Pass Filter

Two identical averagers (i.e. multiplication-less low-pass filters) are used to reduce the unwanted frequencies generated by the square-wave generator. Figure 4 shows the power spectrum obtained after low-pass filtering.

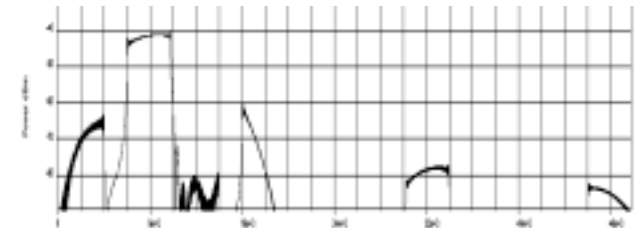


Figure 4 : Low-pass filter output spectrum

3.5 “One-Bit” balanced Quadri-Correlator

The Balanced Quadri-Correlator presented in [7] and further developed in [5] shows a practical and advantageous solution to the computation of $\omega(t)$. Its simplified bloc diagram is shown on Fig. 5.

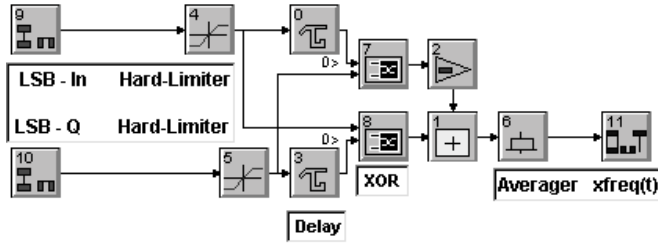


Figure 5 : “One-Bit” balanced Quadri-Correlator (OBBQC)

3.6 Averager

From straightforward analysis [7], the average value of the adder’s output (1) is related to the low-side band in-phase and quadrature (LSB-In and LSB-Q respectively) input signal by a linear relationship (in the form of a variable duty-cycle!). From extensive computer simulations, it has been determined that the “unwanted” frequency components are above 2 kHz. Therefore, the averager must be effective from this frequency and above. The latter is illustrated on Fig. 6 and 7. In this test, the input signal frequency $x_{in}(t)$ is an FSK type signal ($freq_{low} = 200$ Hz, $freq_{high} = 4$ kHz) driven by a square-wave of 185 Hz (symmetrical). Hence, the strongest spectral line is at 185 Hz while the second strongest one is at $3 \cdot 185$ Hz (13 dB weaker).



Figure 6 : Power Spectrum at OBBQC output in 2 tone test

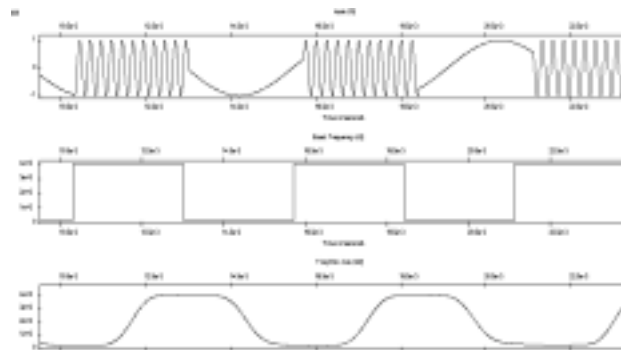


Figure 7 : $x_{in}(t)$, freq. Of $x_{in}(t)$ and estimated frequency

4. SIMULATION RESULTS

4.1 Slow varying frequency tracking error

Figure 8 shows the frequency estimation error of an input signal whose frequency slowly varies between 200 Hz and 4 kHz (top).

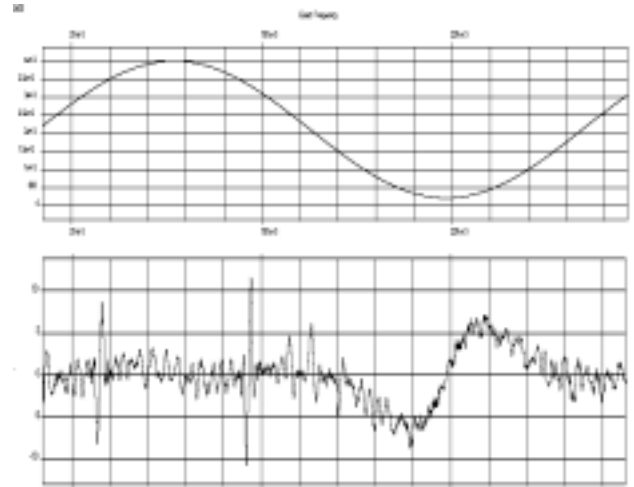


Figure 8 : Input signal frequency (top), $freq_{error}$

The measured RMS frequency errors can be summarized as follows:

- 200 Hz \rightarrow 4000 Hz : 2.99 Hz
- 400 Hz \rightarrow 3000 Hz : 1.82 Hz
- 800 Hz \rightarrow 2400 Hz : 1.36 Hz

4.2 Fast varying frequency

The test signal chosen is of the same type as in section 3.6. Figure 9 shows the input signal frequency (dotted line) and the estimated frequency (continuous line). From this plot, we see that: τ_g (group delay) = 3 ms and $\tau_{trans}(10\% \rightarrow 90\%) = 2.5$ ms.

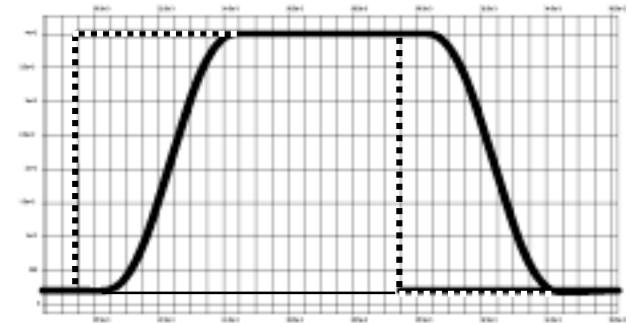


Figure 9 : Input and estimated signal frequency

Note that without dramatically changing the overall system performances and hardware, the reduction of the output averager lengths by factors two will increase the RMS frequency error from 3 Hz to 5 Hz while reducing τ_g and τ_{trans} down to 1.85 and 1.25 ms respectively.

4.3 Sinusoidal Signal and Gaussian Noise

Due to the hard-limiters present at the “One-Bit” balanced Quadri-Correlator inputs, a sinusoidal signal frequency can be accurately estimated if the input signal-to-noise ratio (SNR) due

to uniformly distributed Gaussian noise (0 to 4 kHz) is larger or equal to 10 dB. This is illustrated in Fig. 10

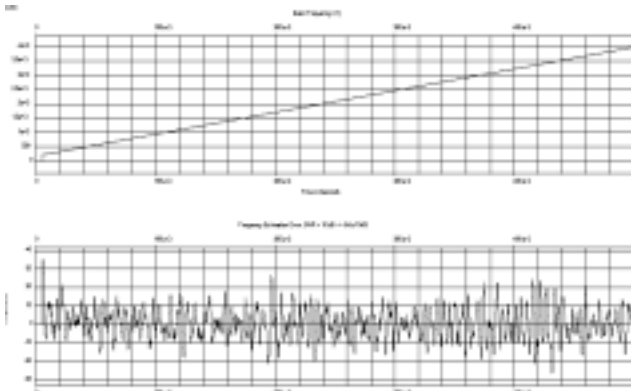


Figure 10: Sinusoidal Input Signal Frequency (top), Frequency Estimation Error (bottom)

From the simulations, the following were measured:

SNR = 10 dB → Frequency Estimation Error = 8.0 Hz (RMS)

SNR = 16 dB → Frequency Estimation Error = 4.4 Hz (RMS)

4.4 Two sinusoidal varying frequency signals

In the case of two sinusoidal varying frequency signals, a minimum of 6 dB between the signal amplitude whose frequency has to be estimated and the other one is necessary to successfully perform the frequency estimation. This is shown on the next two figures. In Fig. 11, the strongest signal (+6 dB) has a frequency which has a sinusoidal shape. In Fig.12, the strongest signal (+6 dB) has a frequency which has the shape of a saw-tooth. Both signal frequencies cover the 200 Hz to 4 kHz system range with a different rate.

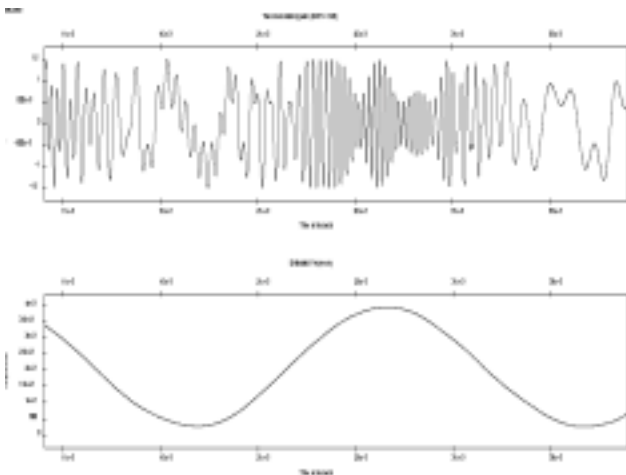


Figure 11: Top: Input signal (Sinus. Freq. Mod + 6dB) Bottom : Frequency Estimation

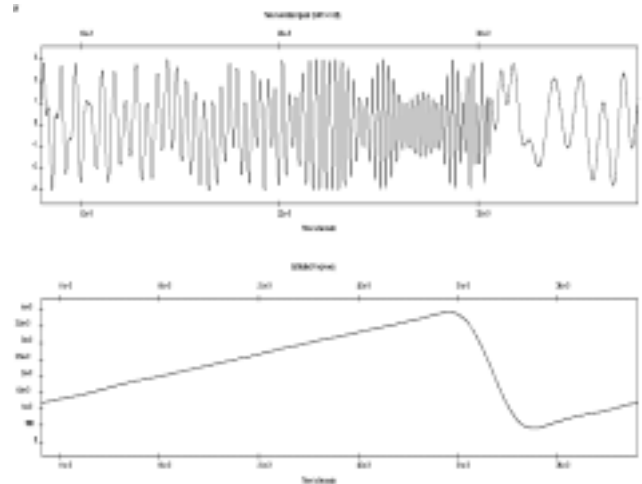


Figure 11: Top: Input signal (Saw-Tooth Freq. Mod + 6dB) Bottom : Frequency Estimation

4.5 Impulsive noise

The original One-Bit” signal processing technique implementation of the *Balanced Quadri-Correlator* provides a design that is inherently robust to impulsive noise and/or abrupt amplitude changes of the input signal. This is best illustrated by Fig. 12.

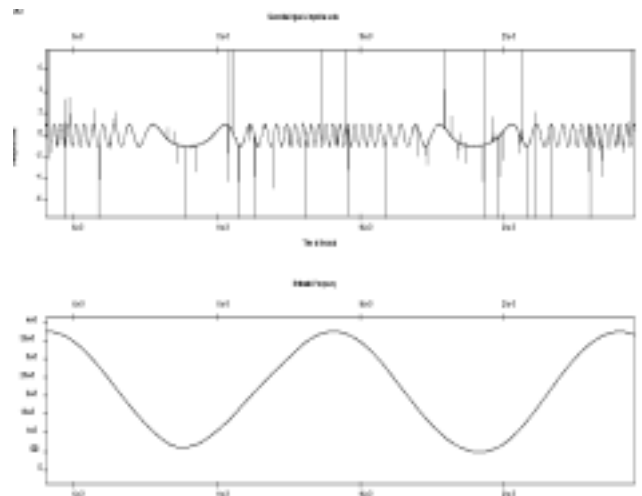


Figure 12: Top: Input signal + impulsive noise Bottom: Frequency Estimation

Fig. 13 shows the insensitivity of the estimator to random input signal amplitude changes.

4.5 Instantaneous Envelope Estimation

A careful analysis of Fig. 1 shows that the instantaneous signal envelope estimation information is readily available from one of the LSB output signals without complex computations (i.e. rectifier followed by averagers) ! This is clearly confirmed by Figure 13.

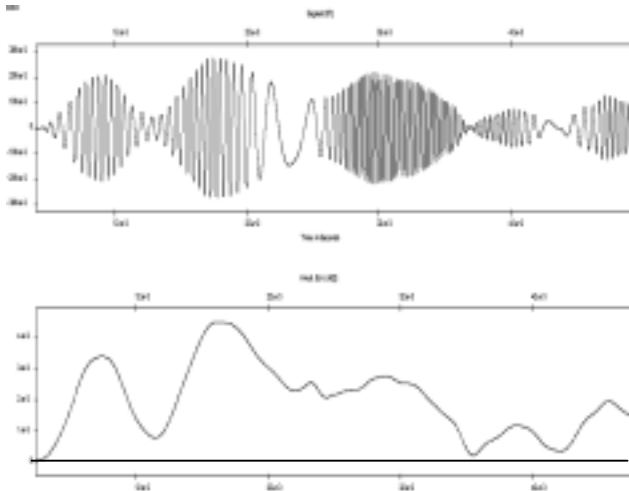


Figure 13: Top: Input signal, Bottom: Envelope Estimation

5. CONCLUSIONS

This paper describes a new *Real-Time Digital Frequency Estimator*. The first series of computer simulations (SystemView) show the very good dynamic performances of the proposed new scheme and no measurable degradations in comparison with the *Arctan* function solution. It is also very robust against impulsive or burst type noise. Furthermore, the instantaneous envelope estimation information is readily available from one of the IF signals without complex computations.

The author persistence to come-up with a *100% multiplication-free* solution has certainly paid-off. It has generated the solution which has the advantages of being both inexpensive and effective, at reasonable cost, in either low power consumption designs or high frequency applications.

Moreover, key aspects of this design (Hilbert Transform Applications) have been largely investigated and developed in relation to Ultra-Sound based R&D projects [8]. Additionally, it has recently been successfully applied to the dynamic speed measurement of very small electrical motors.

Several application oriented extensions of this work can be considered. For instance, a much broader frequency spectrum could be covered by simultaneously using several of these Hilbert Transform based frequency estimators coupled to a "smart" combiner.

6. REFERENCES

- [1] Rick Lyons, "The Discrete Hilbert Transform: A Brief Tutorial", W236, *ICSPAT 99, Orlando, Florida, USA*
- [2] S. Braun and M. Feldman, "Time-Frequency Characteristics of Non-Linear System", *Mechanical Systems and Signal Processing (1997)*, 611-620

- [3] M. Feldman, "Non-Linear System Vibration Analysis using Hilbert Transform, Free Vibration Analysis Method FREEVIB", *Mechanical Systems and Signal Processing (1994)*, 119-127
- [4] M. Feldman, "Non-Linear Free Vibration Identification via the Hilbert Transform", *Journal of Sound and Vibration (1997)*, 475-489
- [5] J-P. Sandoz, C Donzelot, "Computer Simulation of a Digital One-Bit based, Balanced Quadricorrelator Applied to multi-Level FSK Demodulator", *ICSPAT 99, Orlando, Florida, USA*
- [6] S. Baert, L. Roussel-Galle, "RF Speech Clipper with Audio band Hilbert Filter", *Diploma work (2001-2002), University of Applied Sciences of Canton Neuchâtel, Switzerland*
- [7] Floyd M. Gardner, "Properties of Frequency Difference Detectors", *IEEE Trans. Communications*, VOL. COM-33, No. 2, pp. 131-138, Feb. 1985.F.M.
- [8] Miodrag Prokic, MP Interconsulting, 2400, Le Locle, Switzerland. <http://www.mpi-ultrasonics.com>

7. BIBLIOGRAPHY

Jean-Paul Sandoz was born in Neuchâtel, Switzerland, in 1952. He graduated from the Engineering College of Canton Neuchâtel in 1974, and received the B.A.Sc. and M.A.Sc degrees in Electrical Engineering from the University of Ottawa, Canada in 1981 and 1983 respectively.

Between 1975 and 1978, he worked at the Observatory of Neuchâtel, on digital synchronous receivers, Digital Phase-Locked-Loop and geophysical instrumentation. Then he worked a year with EDA Instruments Inc., Toronto, Canada as development engineer. In 1983 and 1984 he was a member of the research staff with Sodeco-Saia, Geneva, Switzerland on projects involving Digital Signal Processing.

He is presently Professor of Analog and Digital Signal Processing at the University of Applied Sciences of Canton Neuchâtel, Switzerland. His teaching and research interests include applied DSP techniques to weak signal detection and classification, nonlinear filtering, low-noise analog front-end, "One-bit" DSP techniques with applications to Phase/Frequency Detectors and Synchronizers, Pulse Response Technique Applications, Active Power Maximization in Transducer, Multiple-Frequencies Locking System, Parameters Adaptation in Time Evolving Processes. He gave several DSP seminars including one in Ujung Pandang, Indonesia.